On a Four Parameter Family of Planar Vector Fields

G. DANGELMAYR & J. GUCKENHEIMER

Communicated by M. GOLUBITSKY

I. Introduction

This paper analyzes the dynamical behavior of a four parameter family of planar vector fields:

$$\begin{aligned} \dot{x} &= y, \\ \dot{y} &= -(x^3 + rx^2 + nx + m) + y(b - x^2). \end{aligned} \tag{1}$$

Our motivation for studying this problem is threefold:

(i) When one fixes $r = m = 0$, the resulting two parameter family is a normal form for a codimension two bifurcation within the class of planar vector fields equivariant with respect to rotation by π. This nilpotent codimension two bifurcation with rotational symmetry occurs frequently in applications and was studied by TAKENS [12]. Our analysis describes the effect of small deviations from symmetry in the system. It provides the type of analysis needed to give a theoretical interpretation of experimental data like those of REHBERG & AHLERS [10]. These authors study codimension two bifurcations in convection of fluid mixtures, but are unable to prevent heat flow through the side walls of the fluid container. The heat flow through side walls is a symmetry breaking bifurcation. However, it is probably appropriate to change the sign of the coefficient of x^3 in (1) to obtain the normal form for the codimension two bifurcation relevant to their study. Thus, our analysis is likely to be only illustrative of the techniques which can be brought to bear on their problem and does not form the basis for a direct comparison.

(ii) The system (1) and its various subsidiary bifurcations occur in simple models of chemical reactors. In particular, the system (1) is closely related to the "cross-shaped diagram" model of BOISSONADE & DE KEPPER [3] for designing oscillating reactors. It also extends the analysis of degenerate bifurcations occurring in the model CSTR equations [5, 6, 14]. Note, however, that the bifurcation we label the Takens-Bogdanov loop occurs in a different form in the CSTR equations and has an unfolding which differs somewhat from the one shown in Figure 3 [b].

(iii) There is a class of bifurcation problems for planar vectorfields which can be studied rigorously by means of perturbation theory for systems which are almost divergence free [2, 8, 13]. System (1) provides one of the most general examples of such problems that can be analyzed with elliptic integrals. By rescaling the variables and parameters in (1) according to the scheme $X = \delta x$, $Y = \delta^2 y$, $R = \delta r$, $N = \delta^2 n$, $M = \delta^3 m$, $B = \delta^2 b$ and $T = \delta^{-1} t$, one obtains the system

$$\begin{aligned} \frac{dX}{dT} &= Y, \\ \frac{dY}{dT} &= -(X^3 + RX^2 + NX + M) + \delta(BY - X^2 Y). \end{aligned} \tag{2}$$

The limit $\delta = 0$ of (2) is a Hamiltonian vector field with trajectories that are level curves of the function

$$E(X, Y) = \frac{Y^2}{2} + \frac{X^4}{4} + \frac{RX^3}{3} + \frac{NX^2}{2} + MX. \tag{3}$$

For small values of δ, the perturbation theory for planar vector fields gives criteria for the existence of periodic orbits and simple bifurcations of the system (2) in terms of integrals over domains bounded by the level curves of (3) [1]. The bulk of this paper involves these calculations, with special attention to the singular values of E because these yield the homoclinic solutions of (2).

II. Background and Results

This section describes our results in terms of a set of *stability diagrams* that show the regions of the four dimensional parameter space near the origin which correspond to specific phase portraits. The boundaries of these regions give parameter values at which *bifurcations* occur. The locus of bifurcations constitutes a stratified set with strata consisting of submanifolds of codimensions one, two, three, and four. The boundary of the strata of codimension k consists of the strata of higher codimension. There are several different types of bifurcations which occur, and we give names to each of these subsidiary bifurcations occurring in the system (1). This section describes the codimension one and two bifurcations, all of which were known previously, and postpones a detailed description of the codimension 3 bifurcations to Section 5.

Given a vector field V, such as the system (1) with all parameters zero, one can seek a family of vector fields containing V which satisfies a *structural stability* criterion. Such a family is called a *versal unfolding* of V. The specification of structural stability criteria is more subtle in these problems than the analogous questions in the singularity theory for smooth mappings. Here we seek to establish a weak form of a structural stability statement for the family (1), namely that the qualitative structure of its stability diagram remains unchanged under perturbation. Some aspects of a theorem establishing structural stability for the family (1) remain unproved, so we formulate the following:

Hypothesis. Let F be the family of vector fields defined by (1). In the space of smooth (C^4), four parameter families of vector fields on $\mathbb{R}^2$, there is a neighborhood U of F such that if G is a family of vector fields in U, then there is a homeomorphism between the parameter spaces of F and G which sends vector fields to topologically equivalent vector fields.

There are relatively few points which remain to be proved in establishing the above hypothesis as a theorem. From a computational point of view, it would suffice to have accurate evaluations of the elliptic integrals (near their singular values) which are involved in calculating the location of certain bifurcations. Additionally, we have not calculated all of the nondegeneracy conditions associated with some of the codimension three bifurcations in the problem. One general issue which arises involves the singular dependence of the elliptic integrals describing the location of periodic orbits as they become homoclinic. To contend with this situation, one would like to have an extension of the singularity theory for smooth functions to functions whose asymptotic expansions involve logarithmic terms in the parameters.

Let us turn from the abstract discussion above to the description of the stability diagram for the system (1). We need a dictionary that establishes the nomenclature for bifurcations of codimension smaller than four which occur in the example. For codimensions one and two, the bifurcations are known and have been described previously. Accordingly, we give here the list of these which occur in the system (1). Diagrams showing unfoldings and phase portraits of the codimension two bifurcations are given by GUCKENHEIMER [5], and GUCKENHEIMER & HOLMES [7] discuss the codimension one bifurcations more fully.

Codimension 1:

Saddle Node: SN. The normal form for a saddle node bifurcation in the plane is

$$\dot{x} = \lambda - x^2,$$
$$\dot{y} = ay, \quad (a \neq 0).$$

This bifurcation describes the simultaneous birth of a pair of equilibrium points as the parameter varies. One equilibrium is a saddle and the other is a stable or unstable node. In terms of singularity theory, the saddle-node is a fold singularity for the set of equilibria.

Hopf Bifurcation: H. The normal form for Hopf bifurcation in the plane is

$$\dot{x} = -y + x(\lambda + a(x^2 + y^2)),$$
$$\dot{y} = x + y(\lambda + a(x^2 + y^2)), \quad (a \neq 0).$$

A family of periodic orbits emerges from an equilibrium as the eigenvalues of the equilibrium cross the imaginary axis at $\lambda = 0$.

Saddle Loop: SL. Saddle loops occur where there is a saddle equilibrium with a homoclinic orbit. Because the system (1) never has more than one saddle point, heteroclinic orbits that connect two saddles do not occur. The unfolding of a saddle loop involves the termination of a family of periodic orbits as its period becomes infinite. There are two topologically distinct saddle loops that occur for planar vector fields, depending upon whether the remaining separatrices lie inside or outside the loop.

Double Cycle: D. Double cycles, or saddle nodes of periodic orbits, occur where there is a periodic orbit whose return map has a simple eigenvalue 1. One then imposes upon the return map conditions like those of the discrete version of the saddle-node. A normal form for the return map is

$$f(x, \lambda) = \lambda + x - x^2.$$

Pitchfork: P. Some of the vector fields in the family (1) are symmetric with respect to rotation of the (x, y) plane by π. In the subfamily of symmetric systems defined by $r = m = 0$, the bifurcation of equilibria occurs through a pitchfork bifurcation in which a pair of new equilibria emerges from an existing one. A normal form for the pitchfork in a family of two dimensional vector fields is

$$\dot{x} = \lambda x \pm x^3,$$
$$\dot{y} = ay, \quad (a \neq 0).$$

Codimension 2:

Cusp: C. The cusp occurs when there is an equilibrium with eigenvalue zero. Additionally, one assumes that in the direction of the zero eigenvector, that a second derivative of the vector field vanishes. A normal form for a family of vector fields with a cusp in the plane is

$$\dot{x} = \lambda_1 + \lambda_2 x \pm x^3,$$
$$\dot{y} = ay, \quad (a \neq 0).$$

Degenerate Hopf Bifurcation: DH. The degenerate Hopf bifurcation occurs when a system can be transformed into the normal form for the Hopf bifurcation, but the coefficient of $(x^2 + y^2)(x\,\partial_x + y\,\partial_y)$ in the Hopf normal form is zero. If the coefficient of a corresponding fifth degree term $(x^2 + y^2)^2 (x\,\partial_x + y\,\partial_y)$ is nonzero, then one has the (codimension two) degenerate Hopf bifurcation [13]. In the (λ_1, λ_2) plane there is a region in which the system has a pair of limit cycles. A normal form for the degenerate Hopf bifurcation can be given in polar coordinates as

$$\dot{r} = \lambda_1 r + \lambda_2 r^3 + ar^5 + \ldots, \quad (a \neq 0),$$
$$\dot{\theta} = 1 + \ldots$$

Takens-Bogdanov Bifurcation: TB. The Takens-Bogdanov bifurcation [12] occurs in planar vector fields which have an equilibrium with a nilpotent linearization. A normal form is

$$\dot{x} = y,$$
$$\dot{y} = \lambda_1 + \lambda_2 x + x^2 + xy.$$

As λ_1 and λ_2 are varied around a circle surrounding the origin, one successively meets a curve of saddle-node bifurcations, a Hopf bifurcation curve, a saddle loop bifurcation curve, and another saddle-node bifurcation curve. The analysis which yielded the stability diagram for this bifurcation is a prototype for the calculations reported later in this paper.

Neutral Saddle Loop (NL). The stability of the cycles which appear in the saddle-loop bifurcation is determined by the sum of the eigenvalues at the saddle

point in the loop. When a saddle loop occurs at a saddle point having eigenvalues of equal magnitude, we describe the situation as a neutral saddle loop. In a generic two parameter family, the "Melnikov function" describing the separation between stable and unstable manifolds of a saddle along a transversal to the flow and the sum of the eigenvalues at the saddle are quantities which vary in a nonsingular manner. From this one can infer the existence of a curve of double loops which terminates at a neutral saddle loop in a generic two parameter family. The perturbation calculations of Section 5 include a proof of this fact.

Double Saddle Loop (DL). The double saddle loop occurs when there is a saddle point for which both branches of the unstable manifold are homoclinic trajectories. In a generic two parameter family, the Melnikov functions of the two loops form a nonsingular mapping from the system parameters to $\mathbb{R}^2$. By using the divergence criterion for the existence of periodic orbits and saddle-loops, it follows that there are three curves of saddle loop bifurcations which pass through a point of parameter space when a double loop bifurcation takes place in a generic two parameter family of flows.

Saddle Node Loop (SNL). At a saddle node bifurcation there are three separatrices, two of which bound a region of trajectories asymptotic to the equilibrium. If two of the separatrices coincide as a homoclinic trajectory, then we say that there is a saddle node loop. There is a smooth curve of saddle nodes in the parameter space of a generic two parameter family containing such a point, and there is a curve of saddle loops which terminates there. SCHECHTER [11] analyzes this bifurcation and shows that the curve of saddle loops meets the curve of saddle nodes with quadratic tangency. Thus saddle-node loops and Takens-Bogdanov bifurcations are the two possible termination points for a curve of saddle loops in a generic two parameter family.

Triple Cycle (T). The triple cycle occurs when the return map for a periodic orbit has a cusp. The analysis of this bifurcation is given by applying singularity theory to the difference between the return map and the identity on a one dimensional transversal to the flow at a point of the cycle.

Transversal Intersections. There are vector fields in the family (1) which have two different degeneracies in different regions of the (x, y) plane. Near the parameter values giving this behavior, there are two transversally intersecting submanifolds in the stability diagrams that describe the loci of codimension one bifurcations. In Section § 3 below, we have calculated those transversal intersections which involve two Hopf bifurcations (called Hopf-Hopf), the simultaneous presence of a Hopf and saddle-node bifurcation (Hopf-Saddle Node), and the simultaneous presence of a Hopf bifurcation with a saddle loop (Hopf-Saddle Loop).

Symmetric Nilpotent Bifurcation (SNB). In addition to the codimension two bifurcations described above, there is a codimension two bifurcation of systems with a symmetry that plays a central role here. In the space of vector fields which are equivariant with respect to rotation by π in the plane, there is a codimension two bifurcation of a vector field with an equilibrium having a nilpotent linearization. The normal form of this bifurcation is

$$\dot{x} = y,$$
$$\dot{y} = -\lambda_1 x + \lambda_2 y + ax^3 + bx^2 y, \quad (a \neq 0, b \neq 0).$$

By rescaling the variables in this system, one can set a and b to have magnitude one. Reversing time and reflecting one of the variables changes the signs of λ_2 and b. The two cases $a < 0$ and $a > 0$ are thoroughly distinct. Here we examine only the case $a = -1$, and set $b = -1$ so that orbits near infinity spiral towards the origin.

The stability diagram of this family is depicted in Figure 1 [12]. The main task of this paper is the computation of the stability diagrams for perturbations of this family which occur when the symmetry condition is dropped. We treat this problem in terms of the four parameter family of vector fields (1) by fixing the values of r and m, and then describing the stability diagram of the family depending on n and b. Different regions near the origin in the (r, m) plane lead to different stability diagrams. Thus we present a picture of the (r, m) plane divided into sectors when we plot r^3 versus m. For each of the sectors, there is a stability diagram for a two parameter family in which the only bifurcations occurring are the codimension one and two bifurcations described above together with transversal coincidences of codimension one bifurcations that do not interact with one another. Along the boundaries of the sectors in the (r^3, m) plane, there are values of (b, n) which give codimension three bifurcations of various types. These are discussed more fully in Section 6.

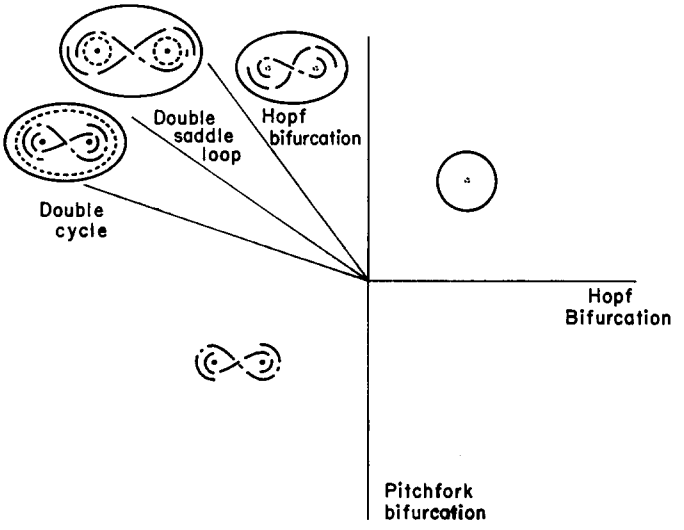

Fig. 1. Stability diagrams for the two parameter symmetric family of vector fields. Phase portraits are coded as follows: stable equilibria are solid dots, unstable equilibria are broken dots, stable limit cycles are unbroken curves, unstable limit cycles are broken curves, unstable separatrices are curves broken into long segments, and stable separatrices are curves broken into long-short segments.

Figures 2a–g present the stability diagrams discussed above. These diagrams should be compared with the stability diagram for the equivariant codimension two bifurcation. Note that three of the bifurcations in the stability diagram for the equivariant family are degenerate when the symmetry is dropped: (1) pitchfork bifurcations perturb to one or three saddle-node bifurcations depending upon

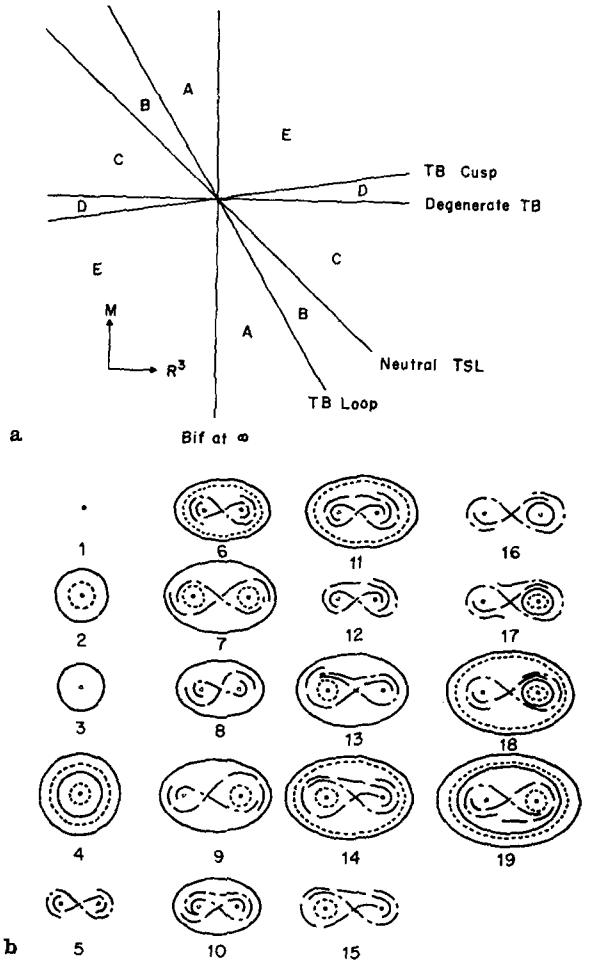

Fig. 2a–b

Fig. 2a–g. Stability diagrams for the four parameter family of vector fields (2). The diagrams are presented as follows. Figure 2a shows the (R, M) plane divided into regions that are bounded by curves along which codimension three bifurcations occur. Codimension three bifurcations involving only transversal crossings of lower codimension bifurcations are not displayed. Figures 2c–2g show the stability diagrams in the (N, B) plane for values of (R, M) in the corresponding region of Figure 2. The numbers correspond to phase portraits shown in Figure 2b. The curves of saddle nodes are thin solid lines, double cycles are heavy solid lines, saddle loops are lines broken in short segments, and Hopf bifurcations are lines broken into long segments. The coding of phase portraits is the same as in Figure 1.

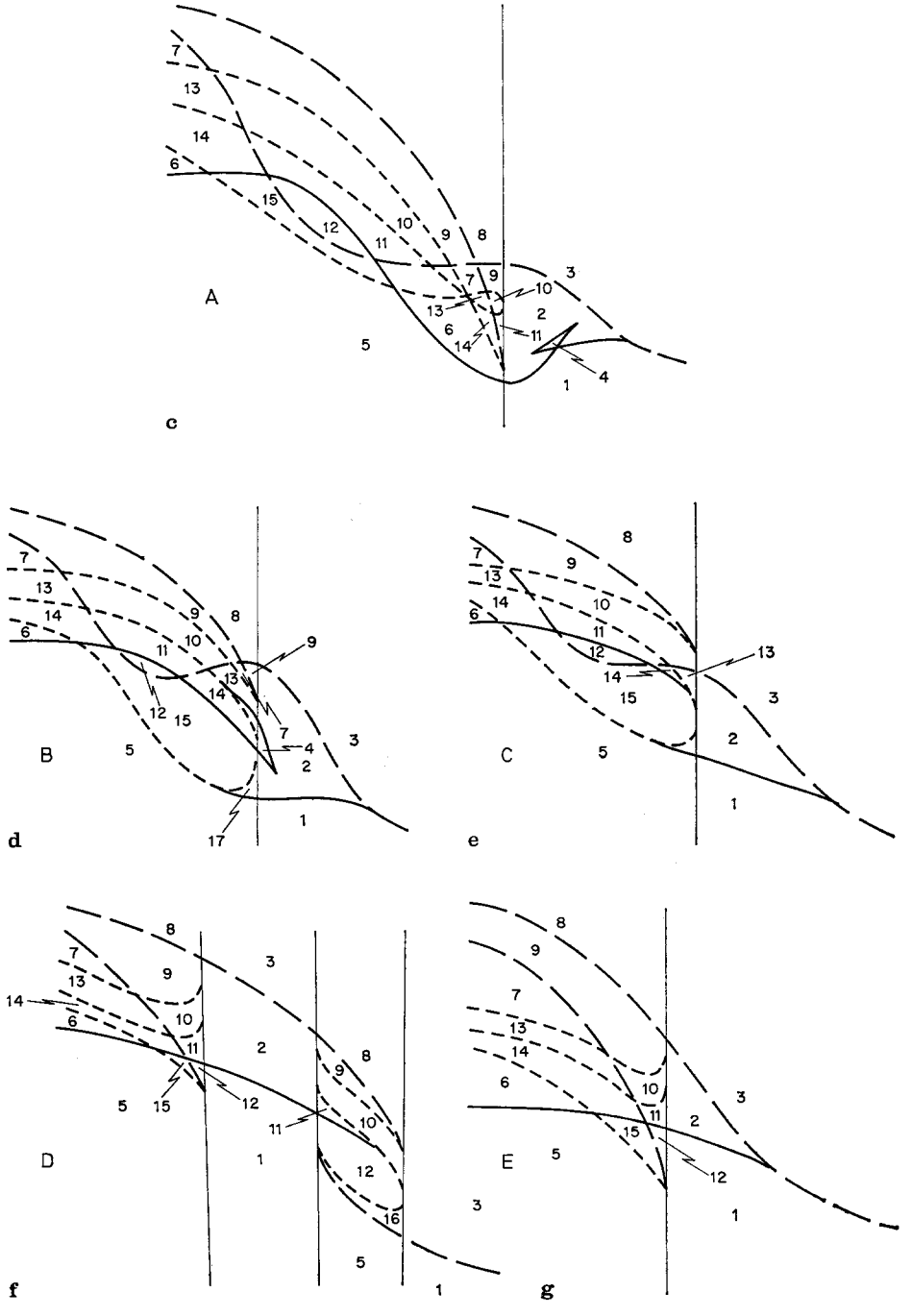

Fig. 2c–g

whether there is hysteresis [5]; (2) the coincident Hopf bifurcations at the nonzero equilibria occur at different parameter values; (3) the double saddle loop splits into three separate saddle-loop curves as shown in the stability diagram of the double saddle loop codimension two bifurcation. These observations give one information about what the perturbed stability diagrams look like far from the origin. Near the pitchfork curve will be one or three curves of saddle-nodes. There will be two curves in the (n, b) stability diagrams for the family (1) which extend to infinity on the left and represent Hopf bifurcations of the left and right equilibria. Below these Hopf bifurcation curves in the (n, b) plane will be three curves of saddle-loops, and below these will be a curve of parameter values corresponding to double cycles. There will be a single curve of Hopf bifurcations extending to infinity on the right.

The connections among all the bifurcation curves near the origin in the (n, b) stability diagrams is quite intricate. Our main result is the following.

Theorem. *From the assumption of the structural stability hypothesis formulated above for the family of differential equations* (1), *the stability diagrams of Figures* 2*a–g give its unfolding.*

Part of the proof of this theorem is based upon numerical computation. In several places, which we have been careful to specify, we have relied upon numerical integration of the equations. Some of the algebraic manipulations in our calculations are rather long. Therefore, we have used the symbolic manipulation programs SMP and MACSYMA to help us complete these calculations which would have exceeded our stamina and accuracy with pencil and paper. The next four sections describe the calculations which yield the stability diagrams of the theorem.

III. Elementary Function Calculations

In this section, we consider the bifurcations of system (2) that can be determined by means of calculations involving elementary functions. There are three calculations that fall within this category, each yielding the locus of one type of codimension one bifurcation: (1) saddle-node bifurcations, (2) Hopf bifurcations, and (3) saddle-loop bifurcations. Combinations of these and degeneracies yield several types of higher codimension bifurcations

Saddle-nodes. The saddle-node bifurcations of (2) are given by parameter values for which the cubic polynomial $X^3 + RX^2 + NX + M$ has a double root. If the double root is S and the simple root is P, these give a parametric representation of the bifurcation locus via

$$R(S, P) = -(2S + P),$$

$$N(S, P) = S^2 + 2SP,$$

$$M(S, P) = -S^2P.$$

Expressed in terms of S and R, we have

$$N = -2RS - 3S^2,$$

$$M = RS^2 + 2S^3,$$

or

$$4N^3 + 27M^2 - 18RMN - R^2N^2 + 4R^3M = 0.$$

The saddle-node is nondegenerate in singularity theory terms whenever $P \neq S$. In terms of (R, N, M), $P = S$ implies $3N = R^2$ and $27M = R^3$. In presenting the stability diagrams, it is convenient to set $R = 1$ or, equivalently, to work with the scale invariant parameters N/R^2 and M/R^3 (and B/R^2 which plays no role in the occurrence of saddle-nodes).

Hopf Bifurcations. Hopf bifurcation occurs at an equilibrium (X_0, Y_0) of (2) if it is not a saddle and if $B = X_0^2$. Thus the loci of Hopf bifurcations are easily characterized in terms of the root h of the cubic $X^3 + RX^2 + NX + M$ at which the bifurcation occurs. One has the equations

$$h^3 + Rh^2 + Nh + M = 0,$$

$$B - h^2 = 0,$$

which imply that

$$B(B + N)^2 = (RB + M)^2.$$

There is the additional condition that

$$3h^2 + 2Rh + N = 3B + N + 2Rh > 0.$$

Thus, when $h^3 + Rh^2 + Nh + M$ has 3 real roots, only the smallest and largest yield Hopf bifurcations. Note that when $R = M = 0$, we have $B = 0$ or $B = -N$, the first case occurring when $N > 0$ and the second when $N < 0$.

Placing the equation (2) into normal form at a point of Hopf bifurcation is a straightforward exercise. If the Hopf bifurcation occurs at $x = h$, we set $U = X - h$, obtaining

$$\dot{U} = Y,$$

$$\dot{Y} = -(3h^2 + 2Rh + N)\,U - (3h + R)U^2 - 2\delta hUY - U^3 - \delta U^2 Y.$$

With $\omega = (3h^2 + 2Rh + N)^{1/2}$ and $U = \omega V$, $Y = \omega^2 W$ and a rescaled time $S = \omega T$, we have

$$V' = W,$$

$$W' = -V - qV^2 - pVW - V^3 - aV^2 W,$$

where the prime indicates differentiation with respect to S and

$$q = (3h + R)/\omega, \quad p = 2\delta h, \quad a = \omega\delta.$$

Introduce next the nonlinear change of coordinates

$$V = v - \tfrac{1}{3} q(v^2 + 2w^2) + \tfrac{1}{3} pvw + (\tfrac{1}{2} q^2 - \tfrac{1}{12} p^2 - \tfrac{1}{4}) v^3 + (\tfrac{5}{24} pq + \tfrac{1}{8} a) v^2 w + (\tfrac{5}{12} q^2 + \tfrac{1}{24} p^2 - \tfrac{3}{8}) vw^2,$$

$$W = w - \tfrac{1}{3} p(v^2 - w^2) + \tfrac{2}{3} qvw - (\tfrac{1}{12} pq + \tfrac{1}{4} a) v^3 + (\tfrac{3}{8} + \tfrac{1}{4} q^2 - \tfrac{3}{8} p^2) v^2 w + (\tfrac{13}{24} pq + \tfrac{1}{8} a) vw^2,$$

which transforms the system for (V, W) to the normal form for the Hopf bifurcation

$$v' = w + (Av + Pw)(v^2 + w^2) + O(5),$$

$$w' = -v + (Aw - Pv)(v^2 + w^2) + O(5),$$

where

$$A = \tfrac{1}{8}(pq - a), \qquad P = \tfrac{3}{8} - \tfrac{5}{12} q^2 - \tfrac{1}{24} p^2.$$

The coefficient A of $(v^2 + w^2)(v\,\partial_v + w\,\partial_w)$ determines the stability of the limit cycle created at the Hopf bifurcation. In terms of the original variables, $A = \dfrac{\delta}{3\omega}(3h^2 - N)$. In particular, the sign of A is the same as that of $3B - N$. If $N = 3B$ (or $a = pq$), the Hopf bifurcation is degenerate. In that case, it is appropriate to calculate the normal form up to fifth order. M. Neveling has implemented this calculation for a general class of systems using SMP. We do not write down the (lengthy) expression of the coordinate transformation for our system, but note that the calculations give $C = -5a/48$ in the normal form

$$v' = w + Pw(v^2 + w^2) + (Cv + Qw)(v^2 + w^2)^2 + O(7),$$

$$w' = -v - Pv(v^2 + w^2) + (Cw - Qv)(v^2 + w^2) + O(7).$$

Therefore, the coefficient of $(v^2 + w^2)^2 (v\,\partial_v + w\,\partial_w)$ that determines the stability of the cycles in the degenerate Hopf bifurcation is always negative in our system.

Saddle-loops. The calculations which characterize saddle loops involve trigonometric functions. Assume that there is a saddle point of (2) at $X = S$, $Y = 0$. The polynomial

$$P(X) = \tfrac{1}{2} X^4 + \frac{2R}{3} X^3 + NX^2 + 2MX - 2E$$

has S as a double root when

$$2E = \tfrac{1}{2} S^4 + \frac{2R}{3} S^3 + NS^2 + 2MS.$$

In addition P has two additional real roots $L < S < K$. The saddle-loops of (2) approach the zero level curve of $P(X) + Y^2$ as $\delta \to 0$ and they satisfy

the divergence criterion of ANDRONOV, LEONTOVICH, GORDON, & MAIER [1]:

$$\int_{A_1}^{A_2} (B - X^2)\sqrt{P(X)}\, dX = 0$$

where $A_1, A_2 \in \{L, S, K\}$. For fixed R, N, M, this gives three equations for different choices of the A_i. Thus

$$\int_{L}^{S} (B - X^2)\sqrt{P(X)}\, dX = 0$$

determines *left saddle loops* that lie to the left of the saddle point,

$$\int_{S}^{K} (B - X^2)\sqrt{P(X)}\, dX = 0$$

determines *right saddle loops* that lie to the right of the saddle point, and

$$\int_{L}^{K} (B - X^2)\sqrt{P(X)}\, dX = 0$$

determines *concave saddle loops* which contain saddle separatrices in their interior.

To compute the saddle-loops, it is convenient to make an affine change of coordinates which sends L to -1 and K to 1. Using the quasihomogeneity of the problem, it suffices to consider the case $K - L = 2$, so that the coordinate change is a translation by $d = \dfrac{L + K}{2}$. We set $u = X - d$ and $s = S - d$. Then the left, right and concave loops are given by the zeros of the integrals

$$\int_{-1}^{s} (B - (u + d)^2)(s - u)\sqrt{1 - u^2}\, du,$$

$$\int_{s}^{-1} (B - (u + d)^2)(u - s)\sqrt{1 - u^2}\, du,$$

$$\int_{-1}^{1} (B - (u + d)^2)\,|u - s|\sqrt{1 - u^2}\, du,$$

respectively. Note the absolute value in the third integral. The values of (R, M, N) are given in terms of (s, d) by

$$R = -3d - \frac{3s}{2},$$

$$N = -\tfrac{1}{2} + 3ds + 3d^2 + \frac{s^2}{2},$$

$$M = \frac{d}{2} + \frac{s}{2} - \frac{ds^2}{2} - \frac{3d^2 s}{2} - d^3.$$

Next compute,

$$\int_{-1}^{s} \sqrt{1-u^2}\, du = \frac{\pi}{4} + \sin^{-1} s + \frac{s\sqrt{1-s^2}}{2}$$

and

$$\int_{s}^{1} \sqrt{1-u^2}\, du = \frac{\pi}{4} - \sin^{-1} s - \frac{s\sqrt{1-s^2}}{2},$$

$$\int_{-1}^{s} u\sqrt{1-u^2}\, du = -\tfrac{1}{3}(\sqrt{1-s^2})^3 \quad \text{and} \quad \int_{s}^{1} u\sqrt{1-u^2}\, du = \tfrac{1}{3}(\sqrt{1-s^2})^3,$$

$$\int_{-1}^{s} u^2\sqrt{1-u^2}\, du = \frac{\pi}{16} + \frac{\sin^{-1} s}{8} - \frac{s\sqrt{1-s^2}}{8} + \frac{s^3\sqrt{1-s^2}}{4},$$

and

$$\int_{s}^{1} u^2\sqrt{1-u^2}\, du = \frac{\pi}{16} - \frac{\sin^{-1} s}{8} + \frac{s\sqrt{1-s^2}}{8} - \frac{s^3\sqrt{1-s^2}}{4},$$

$$\int_{-1}^{s} u^3\sqrt{1-u^2}\, du = \tfrac{1}{5}(\sqrt{1-s^2})^5 - \tfrac{1}{3}(\sqrt{1-s^2})^3,$$

and

$$\int_{s}^{1} u^3\sqrt{1-u^2}\, du = -\tfrac{1}{5}(\sqrt{1-s^2})^5 + \tfrac{1}{3}(\sqrt{1-s^2})^3.$$

Let $Q(u) = (u-s)((u+d)^2 - B) = u^3 + a_2u^2 + a_1u + a_0$. Then

$$a_0 = s(b - d^2),$$

$$a_1 = b - 2ds + d^2,$$

$$a_2 = 2d - s.$$

With these values, left, right and concave loops are given by

$$wI - \sqrt{1-s^2}\, J = 0$$

where

$$I = \tfrac{1}{8}s - \tfrac{1}{4}d + \tfrac{1}{2}s\,d^2 - \tfrac{1}{2}sB,$$

$$J = \tfrac{2}{15} + \tfrac{1}{3}d^2 - \tfrac{5}{12}s\,d - \tfrac{7}{120}s^2 + \tfrac{1}{20}s^4 + \tfrac{1}{6}s^3\,d + \tfrac{1}{6}s^2\,d^2 - (\tfrac{1}{3} + \tfrac{1}{6}s^2)B$$

and

$$w = \begin{cases} \dfrac{\pi}{2} - \sin^{-1} s & \text{for right loops,} \\ -\dfrac{\pi}{2} - \sin^{-1} s & \text{for left loops,} \\ -\sin^{-1} s & \text{for concave loops.} \end{cases}$$

This equation can be readily solved for B.

Codimension Two Calculations

There are a number of codimension two bifurcations whose location can be computed in terms of algebraic calculations and the evaluation of elementary integrals. These are enumerated here:

Takens-Bogdanov bifurcation. When there is an equilibrium with nilpotent linearization, Takens-Bogdanov bifurcation occurs. For the system (2), we have already computed the locus of saddle-node bifurcations as being given by

$$4N^3 + 27M^2 - 18RMN - R^2N^2 + 4R^3M = 0$$

with the double root of the cubic at $X = \dfrac{9M - RN}{2R^2 - 6N}$. The linearization at the equilibrium has zero trace if $B = X^2$. Using $3X^2 + 2RX + N = 0$ at the equilibrium, we have

$$R(9M - RN) + (R^2 - 3N)(3B + N) = 0$$

or

$$3RM + R^2B - 3BN - N^2 = 0$$

or

$$B = \frac{(N^2 - 3RM)}{(R^2 - 3N)}.$$

At a Takens-Bogdanov bifurcation, we would like to compute the normal form. This is a simple matter, since a translation along the x-axis leaves the system (2) in the normal form of Bogdanov. Setting

$$s = \frac{9M_0 - RN_0}{2R_0^2 - 6N_0} \quad \text{and} \quad U = X - s,$$

we have

$$\dot{U} = Y,$$

$$\dot{Y} = -(U^3 + (R + 3s)U^2) + \delta Y(B - s^2 - 2sU - U^2).$$

Provided $(R + 3s)$ and s are non-zero, the bifurcation is non-degenerate. If $R + 3s$ is zero, there is a codimension three bifurcation which is the occurrence of a cusp in the locus of equilibria with a nilpotent linearization. When $s = 0$, there is a codimension three bifurcation in which the degree two expansion at the bifurcating equilibrium is divergence free.The unfoldings of these codimension three bifurcations are discussed later.

Coincident Hopf and Saddle-node. It can happen that there is a Hopf bifurcation at one equilibrium and a saddle-node at another. If the saddle-node bifurcation is at $X = s$ and the Hopf bifurcation is at $X = h$, then, combining the equa-

tions derived earlier, we have

$$B = h^2,$$
$$R = -(2s + h),$$
$$N = s^2 + 2sh,$$
$$M = -s^2h.$$

As in the previous examples, one can eliminate s, h from these equations to obtain a pair of equations for the simultaneous occurrence of a Hopf bifurcation and saddle-node. Of special interest to us are situations in which one or the other of these bifurcations is degenerate. If the Hopf bifurcation is degenerate, then $3B = N$ and $\frac{M}{R^3} = -\frac{9}{125}$. If the saddle-node is a point of Takens-Bogdanov bifurcation, then $s = -h$ and $\frac{M}{R^3} = -1$.

Hopf-Hopf bifurcation. For two Hopf bifurcations to occur simultaneously, the equilibria of the system must occur at $X = -h,\ s,\ h$ with $|s| < h$. This yields the equations

$$B = h^2,$$
$$R = -s,$$
$$N = -h^2,$$
$$M = sh^2.$$

Thus the locus of Hopf-Hopf bifurcations is given by $B + N = 0$ and $M - RN = 0$. Since $|s| < h$, we have $\frac{N}{R^2} < -1$ at the Hopf-Hopf bifurcation and $\frac{M}{R^3} < -1$.

Cusps. We have already observed that the set of equilibria has a surface of cusps in the four dimensional parameter space defined by the equations $\frac{M}{R^3} = \frac{1}{27}$, $\frac{N}{R^2} = \frac{1}{9}$.

Double saddle-loops. By use of the notation introduced to discuss saddle loops, the simultaneous occurrence of right and left saddle loops is given by the simultaneous solutions of the equations

$$\left(\frac{\pi}{2} - \sin^{-1} s\right) I - \sqrt{1 - s^2}\, J = 0,$$
$$\left(-\frac{\pi}{2} - \sin^{-1} s\right) I - \sqrt{1 - s^2}\, J = 0.$$

This pair of equations is equivalent to $I = J = 0$. Solving $I = 0$ for B gives

$$B = \tfrac{1}{4} - \frac{d}{2s} + d^2,$$

and substituting this expression into J yields

$$J = \tfrac{1}{6}(1 - s^2)\left(\frac{d}{s} + \tfrac{3}{10}\right) = 0.$$

Therefore, $d = -\dfrac{3s}{10}$ and we obtain a parametric representation of the locus of double saddle loops as

$$\frac{B}{R^2} = \tfrac{1}{4} + \frac{10}{9s^2},$$

$$\frac{N}{R^2} = -\tfrac{13}{36} - \frac{25}{18s^2},$$

$$\frac{M}{R^3} = -\tfrac{7}{36} - \frac{175}{108s^2},$$

with $s \in [-1, 1]$. As $s^2 \to 1$, the limiting value of M/R^3 is $-49/27$. Therefore, double saddle loops occur in the stability diagrams for $\dfrac{M}{R^3} \in [-\infty, -\tfrac{49}{27}]$.

Trace 0 *Saddle-loops.* The calculations of the location of saddle-loops at saddle points where the trace is zero do not produce simple rational expressions like those for the double saddle-loop though the procedures are similar. The condition that the saddle-point have a linearization with trace 0 is

$$B = S^2.$$

Therefore we want to find the zeros of the integrals

$$\int_S^K (S^2 - X^2)(X - S)\sqrt{(X - L)(K - X)}\, dX$$

and

$$\int_L^K (S^2 - X^2)\,|X - S|\sqrt{(X - L)(K - X)}\, dX$$

for the appearance of trace 0 loops to the right of the saddle and for the concave saddle loops, respectively. Once again, set $K - L = 2$, $d = \tfrac{1}{2}(L + K)$ and $s = S - d$. Then the two integrals can be readily computed, yielding d as a function of $s \in [-1, 1]$. Substituting these values for d, we obtain long expressions for M/R^3, N/R^2, B/R^2 along the trace 0 saddle-loop loci in terms of $s \in [-1, 1]$. Numerical tables of $(M/R^3, N/R^2, B/R^2)$ are given in Tables 1 and 2. The final

Table 1. Calculated derivatives giving stability of concave saddle loops with trace zero

M/R^3	N/R^2	B/R^2	Derivative
−1.81481	−1.75	1.36111	−1.25664
−1.70467	−1.65521	1.28539	−0.649234
−1.60087	−1.56514	1.21363	−0.408559
−1.50303	−1.47954	1.14564	−0.22825
−1.41077	−1.39815	1.08121	−0.0792208
−1.32371	−1.3207	1.02013	0.0497853
−1.24147	−1.24691	0.9622	0.164531
−1.1637	−1.1765	0.907235	0.268428
−1.09006	−1.1092	0.855053	0.363691
−1.02021	−1.04473	0.805484	0.451846
−0.953846	−0.982838	0.758366	0.533994
−0.890688	−0.92325	0.713551	0.610954
−0.830462	−0.865705	0.670901	0.683354
−0.772922	−0.809949	0.630289	0.751682
−0.717842	−0.755731	0.591598	0.816323
−0.665016	−0.702807	0.554725	0.877584
−0.614265	−0.650939	0.519577	0.935712
−0.565432	−0.599901	0.48607	0.990906
−0.518386	−0.549478	0.454135	1.04333
−0.473024	−0.499468	0.423713	1.0931
−0.429272	−0.449692	0.394755	1.14034
−0.387082	−0.399993	0.367224	1.18511
−0.34644	−0.350249	0.341092	1.2275
−0.307361	−0.300374	0.316342	1.26753
−0.269888	−0.25033	0.292965	1.30526
−0.234093	−0.200136	0.270959	1.34071
−0.200071	−0.149876	0.250332	1.37389
−0.167934	−0.0997102	0.231092	1.40482
−0.137809	−0.0498808	0.213253	1.4335
−0.109825	−7.19340*^−4	0.196831	1.45993
−0.0841059	0.047352	0.181838	1.48411
−0.0607627	0.0938221	0.168288	1.50602
−0.0398836	0.138099	0.156187	1.52567
−0.021528	0.179526	0.145539	1.54303
−0.00572383	0.217402	0.136343	1.55811
0.00753222	0.25101	0.128591	1.57089
0.0182701	0.279651	0.122273	1.58136
0.0265378	0.302686	0.117378	1.58951
0.0323905	0.319565	0.113892	1.59533
0.0358786	0.329869	0.111806	1.59883

Table 2. Calculated derivatives giving stability of right saddle loops with trace zero

M/R^3	N/R^2	B/R^2	Derivative
−1.81481	−1.75	1.36111	−1.25664
−1.60092	−1.56518	1.21365	−0.851681
−1.41127	−1.39862	1.0814	−0.706483
−1.24339	−1.24873	0.962934	−0.604341
−1.0949	−1.11401	0.856879	−0.524612
−0.963653	−0.993013	0.761982	−0.459271
−0.847673	−0.884396	0.677094	−0.40418
−0.745203	−0.786933	0.601173	−0.356868
−0.654671	−0.699508	0.533282	−0.315717
−0.574683	−0.621108	0.472577	−0.279593
−0.504009	−0.550817	0.418304	−0.247667
−0.44156	−0.487815	0.369787	−0.219309
−0.386376	−0.43136	0.326422	−0.194025
−0.337614	−0.380789	0.287671	−0.17142
−0.294531	−0.335506	0.253053	−0.15117
−0.256471	−0.29498	0.222141	−0.133009
−0.222859	−0.25873	0.194551	−0.11671
−0.193187	−0.22633	0.169941	−0.102082
−0.167008	−0.197395	0.148008	−0.0889583
−0.143929	−0.171582	0.128479	−0.0771953
−0.123601	−0.148581	0.111111	−0.0666667
−0.105718	−0.128116	0.0954859	−0.0572608
−0.0900074	−0.109939	0.0820091	−0.0488784
−0.0762305	−0.0938257	0.0699063	−0.0414305
−0.0641747	−0.0795763	0.0592212	−0.0348368
−0.0536517	−0.0670102	0.0498136	−0.0290246
−0.0444948	−0.0559652	0.0415578	−0.0239278
−0.0365559	−0.0462949	0.0343406	−0.0194857
−0.0297034	−0.0378676	0.0280606	−0.0156422
−0.0238204	−0.0305646	0.0226263	−0.0123458
−0.0188027	−0.0242785	0.0179554	−0.00954824
−0.0145576	−0.0189126	0.0139738	−0.00720437
−0.0110025	−0.0143794	0.0106146	−0.00527175
−0.00806349	−0.0105997	0.0078175	−0.00371004
−0.00567479	−0.007502	0.00552802	−0.00248068
−0.00377749	−0.00502137	0.00369696	−0.00154642
−0.00231892	−0.00309911	0.00227981	−8.70767*^−4
−0.00125197	−0.00168196	0.0012363	−4.17389*^−4
−5.34402*^−4	−7.21611*^−4	5.29991*^−4	−1.49083*^−4
−0.563075	−1.74321*^−4	1.27866*^−4	−2.59475*^−5

columns of these tables are the values of the integrals

$$\int_S^K \frac{S+X}{\sqrt{(X-L)(K-X)}}\,dX,$$

$$\int_L^K \frac{(S-X)(S+X)}{|S-X|\sqrt{(X-L)(K-X)}}\,dX,$$

which give the derivative of the divergence with respect to the Hamiltonian. This determines the stability of the homoclinic orbits.

For the purpose of drawing qualitative pictures of the stability diagrams, we use the numerical calculations in Tables 1 and 2 to make the following assumptions. First, we assume that the left and concave trace 0 saddle-loops occur for $\frac{M}{R^3} \in [-\frac{49}{27}, 0]$ and $\frac{M}{R^3} \in [-\frac{49}{27}, \frac{1}{27}]$ respectively. The loops which occur to the right of the saddle are all unstable, while the concave loops are neutrally stable for a value of $\frac{M}{R^3} \approx -1.358$. For larger values of $\frac{M}{R^3}$, the loops are stable, while for smaller values, they are unstable. The limit value $\frac{M}{R^3} = -\frac{49}{27}$ corresponds to the codimension three bifurcation with a loop formed from the two separatrices of the degenerate singular point. This bifurcation is discussed in detail in Section 5. Some additional information and details of the numerical calculations are presented in the Appendix.

Saddle-loop and Hopf bifurcations. Calculations similar to those for finding trace 0 saddle-loops locate the occurrence of saddle-loops which occur simultaneously with Hopf bifurcations. One merely fixes B at the value giving Hopf bifurcation rather than the value giving trace 0 at the saddle-point. These are independent phenomena happening in different parts of the phase plane, so stability diagrams associated with this codimension two bifurcation have merely transversal intersections of the Hopf and saddle-loop loci. The computation of these bifurcations indicates that there are parameter ranges of M/R^3 for which some bifurcation curves have multiple crossings. These multiple crossings are not implied by the topology of the stability diagrams near other points of codimension two or three bifurcation.

IV. Elliptic Integral Calculations

This section describes the elliptic integral calculations that yield the locations of periodic orbits and their bifurcations in the system (2) for small values of δ. Due to the length of the expressions that need to be evaluated and the difficulty of obtaining accurate evaluations of the elliptic integrals near their singular values, the numerical determination of the bifurcation curves for double loops is much less complete than the results of the previous sections. Both SMP and MACSYMA have been used for calculations in this section.

The divergence criterion of ANDRONOV, LEONTOVICH, GORDON & MAIER [1] states that a necessary condition for the existence of a continuous family of periodic orbits of (2) depending on δ and approaching Γ as $\delta \to 0$ is that Γ be contained in a level curve of E and that

$$\int_{\text{Int}\,\Gamma} (B - X^2)\, dX\, dY = 0.$$

Integrating with respect to Y gives

$$2 \int_{A_1}^{A_2} (B - X^2)\, Y\, dX = 0 \tag{Ex}$$

where $Y = \left(2E - 2MX - NX^2 - \frac{2RX^3}{3} - \frac{X^4}{2}\right)^{1/2}$ and A_1 and A_2 are the intersections of Γ with the X-axis. The integral (Ex) is an elliptic integral and can be reduced by the classical procedure of Legendre to a linear combination of $I_0 = \int \frac{dX}{Y}$, $I_1 = \int \frac{X}{Y}\, dX$, and $I_2 = \int \frac{X^2}{Y}\, dX$ whose coefficients are polynomials in (B, E, M, N, R). Further (fractional-linear) changes of coordinates place the roots of Y at ± 1 and $\pm k$ to yield the standard elliptic integrals.

The stability of the periodic orbits determined by solving the equation (Ex) is found by differentiating this equation with respect to E. Derivatives which are negative yield stable cycles for $\delta > 0$ in (2), while positive derivatives give unstable cycles and zero derivative indicates neutral stability. Since $\frac{\partial Y}{\partial E} = \frac{1}{Y}$, the equation yielding neutrally stable cycles is

$$\int_{A_1}^{A_2} \frac{B - X^2}{Y}\, dX = 0 \tag{NS}$$

or $BI_0 = I_2$ in terms of the elliptic integrals introduced above.

Working with the roots A_i of the polynomial

$$P(X) = -\tfrac{1}{2} X^4 - \frac{2R}{3} X^3 - NX^2 - 2MX + 2E = -\tfrac{1}{2} \prod_{i=1}^{4} (X - A_i),$$

we derive explicit expressions that parametrize the solutions of the pair of equations (Ex) and (NS). To accomplish this, we perform an affine change of coordinates that sends (A_1, A_2) to $(-1, 1)$ and use the location of the remaining two roots in the new coordinate system as parameters. By exploiting the quasihomogeneity of the system (2), these calculations are simplified by assuming $A_2 - A_1 = 2$. Additionally, the two roots of P not equal to ± 1 can be transformed to lie at $\pm k$. Using k and a parameter q of this coordinate transformation, we express the condition for double cycles to exist in terms of standard elliptic integrals.

Take now $A_2 - A_1 = 2$ and define

$$d = \tfrac{1}{2}(A_1 + A_2),$$

$$X = U + d.$$

Let s_1 and s_2 be the roots $A_3 - d$, $A_4 - d$ of the polynomial $P(X)$ translated to the U coordinate system. Substituting into P, (Ex), and (NS) we obtain (1) a system of equations expressing (E, R, N, M) in terms of (d, s_1, s_2) and (2) a pair of equations for giving the location of double cycles as polynomial expressions in (B, d, s_1, s_2) and the integrals

$$J_i = \int_{-1}^{1} \frac{U^i}{Y}\, dU, \qquad i = 0, 1, 2.$$

Now consider the dependence of (NS) and (Ex) on (B, d). Since $P = Y^2$ is independent of (B, d), both equations are linear in B and quadratic in d. Closer inspection shows that the equations depend linearly on the parameters $B + d^2$ and d. Therefore, this pair of equations can be solved explicitly for B and d in terms of the s_i and elliptic integrals J_i. In principle, the outcome is (approximately) a parametrization of $(E/R^4, M/R^3, N/R^2, B/R^2)$ along the surface of double cycles in terms of (s_1, s_2). However, the accurate evaluation of the J_i's is complicated by the presence of poles of the integrand near the interval $[-1, 1]$ for many parameter values of interest.

A fractional linear transformation which has fixed points at -1 and 1 has the form $v = \dfrac{u+q}{1+qu}$ or $u = \dfrac{v-q}{1-qv}$. To parametrize the locus of double cycles in terms of standard elliptic integrals, we want to express s_1, s_2 of the u coordinates as the transforms of $\pm k$ in the v coordinates for a suitable value of q. In other words, starting with (k, q) we associate to it the polynomial P (in u coordinates) with roots $\left(\pm 1, \dfrac{\pm k - q}{1 \mp qk}\right)$. Next one uses the Legendre transformations to express the elliptic integrals J_0, J_1, J_2 in terms of standard elliptic integrals. The results of these computations when the roots are $\pm ik$ are

$$J_0 = \int_{-1}^{1} \frac{du}{y} = \sqrt{\frac{1+k^2q^2}{1-q^2}} \int_{-1}^{1} \frac{dv}{y},$$

$$J_1 = \int_{-1}^{1} \frac{u\, du}{y} = -\frac{1}{q}\sqrt{\frac{1+k^2q^2}{1-q^2}} \int_{-1}^{1} \frac{dv}{y} + \frac{\sqrt{(1+k^2q^2)(1-q^2)}}{q} \int_{-1}^{1} \frac{dv}{(1-q^2v^2)\, y},$$

$$J_2 = \int_{-1}^{1} \frac{u^2\, du}{y} = \sqrt{\frac{1+k^2q^2}{1-q^2}} \int_{-1}^{1} \frac{dv}{y} - (1+k^2)\sqrt{\frac{1-q^2}{1+k^2q^2}} \int_{-1}^{1} \frac{dv}{(1-q^2v^2)\, y} + k^2(1+k^2)\sqrt{(1-q^2)(1+k^2q^2)} \int_{-1}^{1} \frac{dv}{(v^2+k^2)\, y},$$

$$y^2 = (1-v^2)(v^2+k^2).$$

The expression of $(E/R^4, M/R^3, N/R^2, B/R^2)$ in terms of q, k and the three complete elliptic integrals appearing above is long. The results of SMP calculations are available from us on request. Our efforts at evaluating these expressions numerically have not been successful yet. The "interesting" regions in which triple and quadruple cycles occur apparently lie very close to parameter values for which the elliptic integrals are singular ($|q| \approx 1$ or $k \approx 0$). Further efforts to deal with the resulting numerical difficulties will be described elsewhere. We have also used MACSYMA to compute the equations which describe triple and quadruple loops in terms of s_1 and s_2 when these are complex $s \pm it$. The expressions produced by MACSYMA are very long (hundreds of terms), making it impractical to seek a solution of these equations directly. Consequently, the existence of the quadrupole cycle and the location of the curves of double cycles in the stability diagrams have been determined by a combination of direct numerical integrations of (2) and arguments based upon the unfoldings of the codimension two and three subsidiary bifurcations. This is the weakest part of the analysis in our study.

V. Codimension 3 Bifurcations

This section describes several of the codimension three bifurcations and their unfoldings which occur in the family of vector fields (1). We concentrate attention on those codimension three bifurcations which involve more than the transversal crossing of lower codimension bifurcations in different regions of the phase plane. There are five situations of this type that we examine. These are

(1) Takens-Bogdanov loop: the separatrices at a point of Takens-Bogdanov bifurcation are homoclinic.
(2) Neutral trace 0 saddle: a homoclinic orbit of neutral stability occurs when the saddle point has trace zero.
(3) Degenerate Takens-Bogdanov bifurcation: one of the quadratic coefficients in the Takens-Bogdanov normal form vanishes.
(4) Takens-Bogdanov cusp: the other quadratic coefficient in the Takens-Bogdanov normal form vanishes.
(5) Bifurcation at Infinity: some points of codimension two bifurcation tend to infinity.

Takens-Bogdanov Loop

The Takens-Bogdanov bifurcation for the system (2) occurs near the parameter values $M/R^3 = -49/27$ when δ is small. At a Takens-Bogdanov bifurcation, there is one stable and one unstable saddle separatrix. The codimension three bifurcation described here occurs when these separatrices coincide as a homoclinic orbit. To compute the parameter values at which this occurs, we normalize by setting the Takens-Bogdanov equilibrium point at -1. Then $B = 1$,

and we need to solve the equation

$$\int_{-1}^{1} (1 - X^2) \sqrt{((X+1)^3 (K - X))}\, dX = 0$$

for K to find the intersection of the homoclinic loop with the X-axis. We calculate $K = \frac{13}{7}$, so that R, N, M are the coefficients of

$$\tfrac{1}{4} \frac{d}{dX} ((X+1)^3 (X - \tfrac{13}{7})) = (X+1)^2 (X - \tfrac{8}{7}) = X^3 + \tfrac{6}{7} X^2 - \tfrac{9}{7} X - \tfrac{8}{7}.$$

The unfolding of the Takens-Bogdanov loop is quite complicated. There are two cases which give rise to topologically different stability diagrams, and the more complicated opposite case to the one occurring here can be found in model equations for a stirred tank reactor [6]. Figure 3 gives the stability diagram for our case. To begin the description of the unfolding, we compute the normal form of the Takens-Bogdanov point and the stability of the homoclinic loop. With $V = X + 1$, at the parameter values used above, we have

$$\dot{V} = Y,$$

$$\dot{Y} = + \tfrac{15}{7} V^2 + 2VY - V^3 - V^2 Y.$$

It follows that the small periodic orbits generated from the unfolding of the Takens-Bogdanov bifurcation are unstable. The stability of the homoclinic loop is given by

$$\int_{-1}^{\frac{13}{7}} \frac{1 - X^2}{\sqrt{(1+X)^3 (\frac{13}{7} - X)}}\, dX = \int_{-1}^{\frac{13}{7}} \frac{1 - X}{\sqrt{(1+X)(\frac{13}{7} - X)}}\, dX = \frac{4\pi}{7}.$$

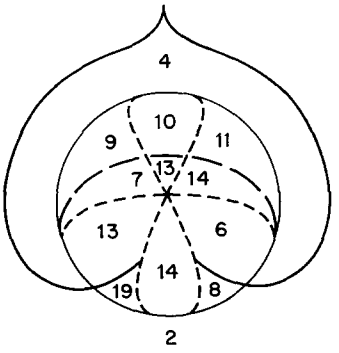

Fig. 3. Stability diagram for a two dimensional sphere in the parameter space surrounding the curve of Takens-Bogdanov loop bifurcations. The numbers correspond to the phase portraits in Figure 2b.

Consequently the homoclinic loop at the Takens-Bogdanov bifurcation is unstable.

The bifurcation locus near the Takens-Bogdanov loop has the topological structure of a cone, so it is determined by its intersection with a small sphere surrounding the point of codimension three bifurcation. Figure 3 illustrates the bifurcations occurring in a two-dimensional sphere which surrounds the locus of the Takens-Bogdanov loop bifurcation in the parameter space. We describe how this diagram was determined. Observe that all four types of codimension one bifurcation occur. The saddle-node locus forms a smooth closed curve because the equilibrium of the Takens-Bogdanov bifurcation is a fold from the singularity theory point of view. The Hopf bifurcations occur along a smooth curve with endpoints of Takens-Bogdanov bifurcation. From the computation of the normal form, we know that the saddle point has positive trace in the region in which small periodic orbits born at these Hopf bifurcations occur.

The saddle-loops represent small homoclinic orbits, large homoclinic orbits lying to the right of the saddle point and large concave homoclinic orbits. The small saddle loops occur along curves which end in saddle node loops. The three curves of saddle node loops must intersect in a double saddle loop since saddle node loops with positive and negative trace at the saddle are possible. Therefore a Takens-Bogdanov bifurcation occurs in each arc of the saddle node locus ending at its intersection with a curve of large saddle loops.

To complete the stability diagram for the Takens-Bogdanov loop, the double cycle bifurcations must be located properly. From each curve of large saddle loop bifurcations, a curve of double cycle bifurcations will begin at points where the saddle point has trace zero. Since the region of small periodic orbits lies between the curve of small saddle loops and the arc of saddle-nodes at which the degenerate equilibrium has a positive eigenvalue, the points of trace zero saddle loops occur on the opposite sides of the double saddle loop point from the Hopf bifurcation curve.

As one crosses the arcs of saddle node bifurcations between the large saddle node loops from the region of one equilibrium to the region of three equilibria, a periodic orbit disappears whose stability agrees with that of the saddle node. Since the Takens-Bogdanov loop is unstable, the arc of negative eigenvalue saddle node bifurcations between large saddle node loops must lie adjacent to a region of parameter space with one equilibrium and three periodic orbits near the Takens-Bogdanov loop. The stable periodic orbit between two unstable ones disappears as the saddle-node curve is crossed. Consequently, the curves of double cycles emanating from the saddle loop curves lie outside the region between the large saddle loops. These curves cross the saddle node bifurcation locus and then separate regions in which there are one and three periodic orbits near the Takens-Bogdanov loop. Since one of the double cycle curves represents the coalescence of the inner periodic orbits and the other double cycle curve represents the coalescence of the outer two of the three periodic orbits, the two curves of double cycles meet in a triple cycle at which all three periodic orbits coalesce.

The discussion above gives the simplest location for the double cycle curves in the stability diagram in the sense that there are the fewest possible structurally stable regions in the stability diagram and the fewest possible periodic orbits.

We have not rigorously established that the stability diagram of Figure 4 is the correct one for the unfolding of the Takens-Bogdanov loop, only that it is the simplest diagram consistent with all of the information about codimension one and two bifurcations known to occur in the unfolding. Note finally that in the system of equations (1) and (2), when a Takens-Bogdanov loop occurs, there is a large stable periodic orbit which plays no role in the unfolding of the Takens-Bogdanov loop. The region of parameter space in which there are four nested periodic orbits appears to be very small, so that it is a delicate numerical computation to exhibit a phase portrait with the four limit cycles.

Neutral Trace 0 Saddle Loop

For parameter values $M/R^3 \approx -1.358$, there is a point along the curve of outer saddle loops at which the saddle point has trace zero and the saddle loop is neutrally stable, *i.e.*, its return map has derivative tending to one as the homoclinic orbit is approached. To analyze the behavior of periodic orbits near this codimension three bifurcation, it is necessary to compute the first few terms in the asymptotic expansion of divergence integrals near a homoclinic orbit. In terms of the Hamiltonian $H(X, Y) = \frac{1}{2} Y^2 + \frac{1}{4} X^4 + \frac{R}{3} X^3 + \frac{N}{2} X^2 + MX = E$ whose level curves approximate the trajectories of (2), the asymptotic expansions are polynomials in $(E - E_0)$ and $\ln (E - E_0)$, E_0 being the value of H at the saddle point. The presence of the logarithmic terms prevents the direct application of results from singularity theory to determine the stability diagrams. Thus we discuss here the "singular singularity theory" appropriate to this example.

Recall the procedure for locating periodic orbits. A family of periodic orbits of (2) approaches a level curve of $H(X, Y)$ as $\delta \to 0$. If the level curve has X intercepts A_1 and A_2 and $P(X) = 2E - 2MX - NX^2 - \frac{2R}{3} X^3 - \frac{1}{2} X^4$, then

$$I(E) = \int_{A_1}^{A_2} (B - X^2) \sqrt{P(X)}\, dX$$

has a zero at the value E of $H(X, Y)$ on the level curve. Stability of the periodic orbits is determined by the sign of

$$\frac{\partial I}{\partial E} = \int_{A_1}^{A_2} \frac{B - X^2}{\sqrt{(P(X))}}\, dX.$$

We want to calculate how the zeros of I depend upon $(N/R^2, M/R^3, B/R^2)$ when we regard $I(E)$ as a family of functions depending upon these parameters. When P has simple roots, I is an analytic function of E and the singularities are folds, cusps and swallowtails. However, when P has a double root, E is a singular value of H and $\frac{\partial I}{\partial E}$ diverges with a logarithmic singularity. This reflects the well known fact that the stability of a homoclinic trajectory is determined by the trace at the saddle point when this trace is non-zero.

In the case of a trace zero saddle point, the coefficient of the lowest order logarithmic term in the expansion of $I(E)$ vanishes. Then $\frac{\partial I}{\partial E}$ is finite and gives the stability of the homoclinic orbit if it is non-zero. In the case of the neutrally stable trace 0 saddle loop, $\frac{\partial I}{\partial E}$ is zero and the lowest order non-zero term in the asymptotic expansion has order $(E - E_0)^2 \ln (E - E_0)$. We now verify that these are indeed the orders of the lowest order terms in the asymptotic expansion and show that perturbations in the family (2) lead to an unfolding.

Consider the asymptotic expansion of the integral I near a saddle point. By translating coordinates so that the saddle point is sent to zero and $e^2 = |E - E_0|$, we obtain integrals of the form

$$J(e) = \int_{c_1(e)}^{c_2(e)} (b_1 + b_2 u + b_3 u^2) \sqrt{-e^2 + a_2 u^2 + a_3 u^3 + a_4 u^4}\, du$$

where $c_1(e)$ and $c_2(e)$ are roots of the polynomial $-e^2 + a_2 u^2 + a_3 u^3 + a_4 u^2$ and $c_1(0) = 0$. To obtain the asymptotic expansion of $J(e)$ in terms of e, we change variables once more with $u = ev$ and substitute into J to obtain

$$J(e) = \int_{c_1(e)/e}^{c_2(e)/e} e^2(b_1 + b_2 ev + b_3 e^2 v^2)\, v \sqrt{a_2 + a_3 ev + a_4 e^2 v^2 - 1/v^2}\, dv.$$

Next approximate the square root in this expression by

$$\sqrt{a_2 + a_3 ev + a_4 e^2 v^2} - \frac{1}{2v^2 \sqrt{a_2 + a_3 ev + a_4 e^2 v^2}}$$

as v becomes large and note that $c_1(e)/e$ tends to a non-zero limit as $e \to 0$. From this expansion, it follows that $J(e)$ has an expansion in powers of e^2 and $\ln e$. The constant term in the expansion is zero at a saddle loop. The coefficient of $e^2 \ln e$ is zero if $b_1 = 0$, and this occurs when the saddle point has zero trace ($b_1 = B - S^2$ where $X = S$ is the location of the saddle.) In this case, the coefficient of e^2 is given by an integral

$$\int_L^K \frac{(S + X)}{\sqrt{(X - L)(K - X)}}\, dX$$

as described in Section 3. Note that this is an affine function of S, so that the coefficients of $e^2 \ln e$ and e^2 vary in a non-singular way as B and S are varied.

From these asymptotic calculations, it follows easily that the zero sets of $J(e)$ as functions of the parameters are homeomorphic to those of the family of functions

$$l_1 + l_2 e^2 \ln e + l_3 e^2 + e^4 \ln e$$

near the neutrally stable trace zero saddle loop provided that the coefficient of $e^4 \ln e$ in the asymptotic expansion is non-zero. The function $l_1 + l_2 e^2 \ln e$

$+ l_3 e^2 + e^4 \ln e$ has a triple zero along the curve in parameter space given parametrically by

$$\begin{pmatrix} l_1 \\ l_2 \\ l_3 \end{pmatrix} = \begin{pmatrix} -e^4 \ln e - e^4 \\ -4e^2 \ln e - 3e^2 \\ 4e^2 (\ln e)^2 + 3e^2 \ln e + e^2 \end{pmatrix}.$$

This corresponds to a cusp on the surface of double loops in the stability diagram and yields a region of parameter space where there are three nearby periodic orbits.

Degenerate Takens-Bogdanov Bifurcation

When $M = 0$ in the system of equations (2) but $R \neq 0$, a degenerate Takens-Bogdanov bifurcation occurs. This case has been analyzed by DUMORTIER, ROUSSAIRE & SOTOMAYOR [4] and also been called a "cusp" by them. At the origin when $N = 0$, the term which is $X^2 \partial_X$ or $XY \partial_Y$ in the normal form of the Takens-Bogdanov bifurcation of the system (2) has zero coefficient, giving rise to the bifurcation considered here. We described the intersection of a small sphere which surrounds the line $R = 0$ in the parameter space with the bifurcation locus.

The origin is a fold from the point of view of singularity theory, so the locus of saddle-nodes forms a closed smooth curve. In the parameter space, this curve lies approximately on the surface $N^2 = 4M$ and is entirely in the region $M \geqq 0$. For fixed $M > 0$, there is a strip bounded by two vertical saddle node lines in the $B - N$ plane for which there are three equilibrium points of the vector field with the same sign of X. One of the saddle-node lines represents the merging of the two equilibrium points closest to the origin and the other represents the coalescence of the equilibrium points farther from the origin. On each of the saddle-node lines a Takens-Bogdanov bifurcation occurs. The saddle loops and Hopf bifurcations associated with these are well separated. The saddle loop curves terminate in saddle-node loops and the Hopf bifurcation curves extend across the opposite saddle-node line from their origination of Takens-Bogdanov bifurcation points. As always, there is a third curve of saddle-loops lying between the other two. The trace of the saddle point changes sign along this curve because its endpoints lie below the point of Takens-Bogdanov bifurcation on one of the saddle-node curves and above the point of Takens-Bogdanov bifurcation on the other. Consequently, there is a trace 0 saddle-loop along the curve, and the double loop curve terminates there.

To complete a picture of the intersection of a sphere surrounding the line $M = 0$ in the parameter space with the bifurcation locus, we observe that when N is near the line of saddle-nodes far from the origin, the saddle loops surrounding the equilibrium point at the origin are stable. Therefore, when M/R^3 is slightly smaller than zero, there is a point with a trace zero saddle loop that occurs near $N = B = 0$. The branch of small double loops emanating from this point terminates at the degenerate Hopf bifurcation which is also close to zero.

Takens-Bogdanov Cusp

For the parameter values $M/R^3 = 1/27$, there is a cusp of equilibrium points from the point of view of singularity theory. In addition, there is a value of B for which the cusp point has a nilpotent linearization. If one computes the Takens-Bogdanov normal form at this point, the term $X^2\,\partial_Y$ has zero coefficient. This type of codimension three bifurcation occurs in the CSTR model for chemical reactors and has been analyzed in GUCKENHEIMER [5] and MEDVED [9]. We describe here the results of this analysis which yields a picture of the intersection of a small sphere surrounding the curve $M/R^3 = 1/27$ in the parameter space with the bifurcation locus.

First the locus of saddle-node bifurcations contains two cusp points which are the intersections of the sphere with the line of cusps in $B - N$ plane for $M/R^3 = 1/27$. The non-zero eigenvalue is positive at one cusp and negative at the other, so along each of the arcs of saddle nodes joining the cusps there is a Takens-Bogdanov bifurcation. The Hopf bifurcations occur along a curve whose endpoints are the points of Takens-Bogdanov bifurcation. The branches of saddle loops emanating from the Takens-Bogdanov bifurcation do not intersect, and they end at saddle node loops. The remaining branch of saddle nodes lies between these and ends in saddle node loops. The trace of the saddle changes sign. Thus there is a curve of double loops; it has ends at the trace zero saddle loop and at a degenerate Hopf bifurcation.

Bifurcation at Infinity

The transition which occurs in the system (2) as R passes through zero in the parameter space is relatively simple. The points of intersection of the two Hopf curves and the double saddle loop points tend to infinity. Otherwise the stability diagrams on the two sides of the surface $R = 0$ are similar to one another.

Acknowledgments. This research was partially supported by grants from the National Science Foundation (J. G.), the Air Force Office of Scientific Research (J. G. and G. D.) and the Stiftung Volkswagenwerk (G. D.).

Appendix : Additional Calculations for Trace-0-saddle loops

The condition $B = (s + d)^2$ for the trace at a saddle being zero in the persistence condition for saddle loops allows us to solve the resulting equation for d, giving

$$10d = \frac{15w(s - 4s^3) - \sqrt{1 - s^2}\,(16 - 47s^2 - 14s^4)}{3w(1 + 4s^2) - \sqrt{1 - s^2}\,(13s + 2s^3)}.$$

The region in (M, R)-plane in which saddle loops with trace zero exist is determined by the values of

$$\frac{M}{R^3} = \frac{4(d + s)\,(2d^2 + ds - 1)}{27(s + 2d)^3},$$

evaluated along $d = d(s)$ when s varies between -1 and 1. Consider first the case of right loops. The asymptotic behavior of d near $s = -1$ and $s = 1$ has the form

$$d \sim \tfrac{3}{10} - \frac{3}{5\pi}\sqrt{2(1+s)} + O(1+s) \qquad (s \to -1)$$

$$d \sim -1 + \tfrac{5071}{7680}(1-s) + O((1-s)^2) \qquad (s \to 1).$$

We note that near $s = 1$ the leading terms of the numerator and denominator of $d(s)$ are of order $(1-s)^3$; hence the asymptotics of d require expansions up to fourth order. Using this result in M/R^3 gives

$$\frac{M}{R^3} \sim -\tfrac{49}{27} + \frac{1575}{108\pi}\sqrt{2(1+s)} + O((1+s)) \qquad (s \to -1)$$

$$\frac{M}{R^3} \sim -\frac{727911}{3840^2}(1-s)^2 + O((1-s)^3) \qquad (s \to 1).$$

Thus, $M/R^3 \in [-\frac{49}{27}, 0]$ for s near the boundary values ± 1.

Next consider the case of concave loops. Since $w = -\sin^{-1} s$, $d(s)$ is an odd function and $\dfrac{M}{R^3}$ is an even function of s. Consequently it suffices to investigate the asymptotic behavior near $s = 0$ and $s = 1$. We find

$$d \sim \frac{1}{10s} - \frac{3s}{20} + O(s^3) \qquad (s \to 0)$$

$$d \sim \tfrac{3}{10} + \tfrac{31}{50}(1-s) + O((1-s)^{3/2}) \qquad (s \to 1),$$

so that d diverges as $s \to 0$. Substituting these expansions into M/R^3 yields

$$\frac{M}{R^3} \sim \tfrac{1}{27} - \tfrac{50}{27}s^2 + O(s^4) \qquad (s \to 0)$$

$$\frac{M}{R^3} \sim -\tfrac{49}{27} + \tfrac{245}{54}(1-s) + O((1-s)^{3/2}) \qquad (s \to 1).$$

Again, $M/R^3 \in [-\frac{49}{27}, \frac{1}{27}]$ when s is near the boundaries $s = 0$ and $s^2 = 1$.

If we can show that the derivative $\dfrac{d}{ds}(M/R^3)$ does not vanish for $s \in (0, 1)$ and for $s^2 < 1$ in the concave and the right case, then saddle loops with trace 0 exist only in the regions $\dfrac{M}{R^3} \in \left[-\dfrac{49}{26}, \dfrac{1}{27}\right]$ respectively. A calculation using SMP shows that $\dfrac{d}{ds}(M/R^3) = 0$ for some s if and only if the function

$$g(s) \equiv (1-s^2)^{3/2} p_1(s) - 3(1-s^2)\, ws\, p_2(s) - 45\sqrt{1-s^2}\, w^2 p_3(s) + 675 s w^3 p_4(s)$$

has a zero, where

$$p_1(s) = 2048 + 18148s^2 - 3127s^4 + 13618s^6 + 2588s^8 - 200s^{10},$$

$$p_2(s) = 3688 + 15591s^2 + 6176s^4 + 7316s^6 + 336s^8 - 32s^{10},$$

$$p_3(s) = 12 - 247s^2 - 1410s^4 - 432s^6 - 128s^8,$$

$$p_4(s) = 3 - 12s^2 - 4s^4.$$

Consequently, if M/R^3 encounters an extremum, then the equality

$$\frac{\sqrt{1-s^2}}{3sw} = \varphi(s) \equiv \frac{(1-s^2)\,p_2(s) - 225w^2\,p_4(s)}{(1-s^2)\,p_1(s) - 45w^2\,p_3(s)}$$

must be satisfied for some s. Simple estimates show that both the numerator and the denominator of $\varphi(s)$ are positive if $s^2 < 1$. From this we conclude that the equality cannot be satisfied for the concave case because here $sw \leqq 0$. In the case of right loops, the equality cannot hold for $s \leqq 0$, but we were not able to give an analytic proof that $\sqrt{1-s^2}/3sw \neq \varphi(s)$ for $0 < s < 1$. Instead, we have computed numerical values which are presented in Table 3. This table suggests that $\sqrt{1-s^2}/3sw > \varphi(s)$ for $0 \leqq s \leqq 1$.

Table 3

s	$\frac{\sqrt{1-s^2}}{3sw}$	$\varphi(s)$
0.1	2.25524	1.85965
0.2	1.19245	1.15551
0.3	0.83716	0.81332
0.4	0.65883	0.62420
0.5	0.55133	0.50551
0.6	0.47929	0.42484
0.7	0.42754	0.36748
0.8	0.38850	0.32573
0.9	0.35794	0.29495

For determining the loci of concave neutral trace 0 saddle loops we use again the parametrization along saddle loops in terms of the parameters d and s introduced in Subsection III.3. Recall that for concave saddle loops with trace 0 we have

$$10d = \frac{15(s - 4s^3)\sin^{-1} s + \sqrt{1-s^2}\,(16 - 47s^2 - 14s^4)}{3(1 + 4s^2)\sin^{-1} s + \sqrt{1-s^2}\,(13s + 2s^3)}.$$

The derivative of the divergence integrals, evaluated at the loci of concave trace 0 saddle loops, is given by

$$\frac{\partial I}{\partial E} = \left(\int_{-1}^{s} - \int_{s}^{1} \right) \frac{s + 2d + u}{\sqrt{1 - u^2}}\, du$$

$$= 2(s + 2d) \sin^{-1} s - \sqrt{1 - s^2}\,.$$

Solving $\partial I/\partial E = 0$ for d and substituting this into the expression for d above leaves us with a single equation for s,

$$5s(1 - s^2)(13 + 2s^2) - \sqrt{1 - s^2}\,(1 - 42s^2 - 4s^4) \sin^{-1} s - 30s(\sin^{-1} s)^2 = 0.$$

Inspection shows that this equation has a unique solution in $[0, 1]$, given by $s = 0.8850$ with corresponding value for d: $d = -0.2283$. The result $M/R^3 = -1.358$ follows from the expression for M/R^3 as

$$\frac{4(d + s)(2d^2 + ds - 1)}{27(s + 2d)^3}.$$

References

1. A. Andronov, E. Leontovich, I. Gordon, & A. Maier, *The Theory of Bifurcation of Plane Dynamical Systems*, Wiley (New York) (1973).
2. I. Arnold, *On the algebraic unsolvability of Lyapounov stability and the problem of classification of singular points of an analytic system of differential equations*, Funct. Anal. Appl. **4**, 173–180 (1970).
3. J. Boissonade & P. DeKepper, *Transitions from bistability to limit cycle oscillations. Theoretical analysis and experimental evidence in an open chemical system*, J. Phys. Chem. **84**, 501–506 (1980).
4. F. Dumortier, R. Roussaire, & J. Sotomayor, *Generic 3-parameter families of vector filelds on the plane, unfolding a singularity with nilpotent linear part. The cusp case of codimension 3*. Preprint.
5. J. Guckenheimer, *Multiple Bifurcation Problems for Chemical Reactors*, Physica D, **20**, 1–20 (1986).
6. J. Guckenheimer, *Global Bifurcations in Simple Models of a Chemical Reactor*, SIAM Lectures in Appl. Math., **24**, Part 2, 163–174 (1986).
7. J. Guckenheimer & P. Holmes, *Nonlinear Oscillations, Dynamical Systems and Bifurcations of Vector Fields*, Springer-Verlag (New York), 453 pp. (1983).
8. Yu. S. Il'yashenko, *Limit cycles of polynomial vector fields with nondegenerate singular points on the real plane*, Funct. Anal. and Appl. **18**, 199–209 (1984).
9. M. Medved, *The unfoldings of a germ of vector fields in the plane with a singularity of codimension 3*, Czech. Math. J. **35**, 1–42 (1985).
10. I. Rehberg & G. Ahlers, *Experimental observation of a codimension two bifurcation in a binary fluid mixture*, Phys. Rev. Lett. **55**, 500–503 (1985).
11. S. Schechter, *The Saddle-Node Separatrix-Loop Bifurcation*, preprint (1985).
12. F. Takens, *Forced Oscillations and Bifurcations, Applications of Global Analysis*, Communications of Maths. Institute, Rijksuniversiteit, Utrecht, **3**, 1–59 (1974).

13. F. TAKENS, *Unfoldings of certain singularities of vector fields: generalized Hopf bifurcations*, J. Diff. Eq. **14**, 476–493 (1973).
14. D. A. VAGANOV, N. G. SAMOILENKO, & V. G. ABRAMOV, *Periodic regimes of continuous stirred tank reactors*, Chem. Eng. Sci. **33**, 1130–1140 (1978).
15. A. N. VARCHENKO, *Estimate of the number of zeros of an abelian integral depending on a parameter and limit cycle*, Funct. Anal. and Appl. **18**, 99–107 (1984).

Universität Tübingen
and
Cornell University

(Received May 5, 1986)